A rationally designed tyrosine hydroxylase DNA vaccine induces specific antineuroblastoma immunity

Nicole Huebener,[1] Stefan Fest,[1] Anne Strandsby,[1] Elke Michalsky,[2] Robert Preissner,[2] Yan Zeng,[1] Gerhard Gaedicke,[1] and Holger N. Lode[1]

[1]Charité-Universitätsmedizin Berlin, Department of Pediatrics, Campus Virchow, and [2]Charité-Universitätsmedizin Berlin, Institute for Molecular Biology and Bioinformatics, Campus Benjamin Franklin, Berlin, Germany

Abstract

Therapeutic vaccination against tumor antigens without induction of autoimmunity remains a major challenge in cancer immunotherapy. Here, we show for the first time effective therapeutic vaccination followed by suppression of established spontaneous neuroblastoma metastases using a tyrosine hydroxylase (TH) DNA minigene vaccine. We identified three novel mouse TH (mTH3) derived peptides with high predicted binding affinity to MHC class I antigen H2-K^k according to the prediction program SYFPEITHI and computer modeling of epitopes into the MHC class I antigen binding groove. Subsequently, a DNA minigene vaccine was generated based on the expression vector pCMV-F3Ub encoding mutated ubiquitin (Gly^{76} to Ala^{76}) and mTH3. Prophylactic and therapeutic efficacies of this vaccine were established following oral delivery with attenuated *Salmonella typhimurium* SL7207. Only mice immunized with mTH3 were free of spontaneous liver metastases. This effect was clearly dependent on ubiquitin and high affinity of the mTH epitopes to MHC class I antigens. Specifically, we showed a crucial role for minigene expression as a stable ubiquitin-Ala^{76} fusion peptide for vaccine efficacy. The immune response following the mTH3 DNA minigene vaccination was mediated by CD8$^+$ T cells as indicated by infiltration of primary tumors and TH-specific cytolytic activity *in vitro*. Importantly, no cell infiltration was detectable in TH-expressing adrenal medulla, indicating the absence of autoimmunity. In summary, we show effective therapeutic vaccination against neuroblastoma with a novel rationally designed TH minigene vaccine without induction of autoimmunity providing an important baseline for future clinical application of this strategy. [Mol Cancer Ther 2008;7(7):2241–51]

Introduction

To break self-tolerance of the cellular immune system against antigens overexpressed by tumor cells is an important strategy in cancer immunotherapy. A need for the development of such effective additional treatment strategies supporting ''classic'' therapy in pediatric oncology is emphasized in stage IV neuroblastoma. Neuroblastoma, the most common extracranial solid pediatric cancer, is characterized by a dismal prognosis despite novel developments such as high-dose chemotherapy followed by autologous hematopoietic stem cell transplantation, passive immunotherapy (1), and induction of differentiation (2). Thus, the development of a vaccine to activate the cellular arm of the immune system, specifically CD8$^+$ T cells, which seem to be best equipped to eliminate tumor cells, may provide a therapeutic element completing the established neuroblastoma therapy (3, 4).

Neuroblastoma cells are derived from sympathetic neuroblasts and therefore express high amounts of the enzyme tyrosine hydroxylase (TH), the first step enzyme in catecholamine biosynthesis. TH catalyzes the conversion of tyrosine to DOPA, which subsequently leads to the generation of dopamine, norepinephrine, and epinephrine and its metabolites homovanillic acid and vanillylmandelic acid. In fact, catecholamine production and metabolism is a well-established clinical marker for diagnosis and follow-up of neuroblastoma patients (5, 6). Furthermore, microarray analysis of a collection of >70 neuroblastoma tumors revealed a stable expression of TH, which was independent of stage and *MYCN* amplification.[3] Finally, the expression of TH and the downstream tumor-associated biochemical pathway differentiates neuroblastoma from other tissues similar to tyrosinase-driven melanin synthesis in melanoma (7). Based on these considerations, we reasoned that TH may be a useful antigen for vaccination against neuroblastoma.

A critical role for effective vaccination and priming of CD8$^+$ T cells is played by the ''danger signal,'' also provided by the innate immune system (8). Therefore, despite some drawbacks in early human trials (9), DNA vaccination remains a promising approach (10) because it combines high versatility in specific vaccine design with activation of the innate immune system and dendritic cells mediated by Toll-like receptors (11) and stimulated by nonmethylated CpG motifs (12, 13).

Received 1/29/08; revised 3/10/08; accepted 3/15/08.

Grant support: Emmy-Noether-Programm of the Deutsche Forschungsgemeinschaft (Lo635/2) and Fördergesellschaft Kinderkrebs-Neuroblastom-Forschung e.V (H.N. Lode) and Deutsche Krebshilfe (E. Michalsky).

The costs of publication of this article were defrayed in part by the payment of page charges. This article must therefore be hereby marked *advertisement* in accordance with 18 U.S.C. Section 1734 solely to indicate this fact.

Requests for reprints: Holger N. Lode, Charité-Universitätsmedizin Berlin, Department of Pediatrics, Campus Virchow, Augustenburger Platz 1, 13353 Berlin, Germany. Phone: 49-30-450-666233; Fax: 49-30-450-566916. E-mail: holger.lode@charite.de

doi:10.1158/1535-7163.MCT-08-0109

[3] A. Schramm, personal communication.

An important element to enhance the efficacy of a DNA vaccine is the appropriate delivery to the host's immune system. For this purpose, the plasmids encoding a particular immunogen can be applied as an oral vaccine using attenuated, nonreplicating *Salmonella typhimurium* (SL7207) as a carrier to transport the DNA vaccine through the M cells of the gastrointestinal mucosa, which cover secondary lymphoid organs called Peyer's patches (14). Here, the attenuated bacteria are captured by antigen-presenting cells and die due to their mutation, liberating multiple copies of the DNA inside the phagocytes (15). Further activation of the innate and subsequently also the adaptive immune system is mediated by the bacterial cell wall (lipopolysaccharide) and the bacterial DNA (non-methylated CpG motifs), leading to the production of cytokines such as interleukin-1, interleukin-6, or interleukin-12 and other mediators such as nitric oxide, which drive a T_H1-type cellular immune response against the antigen encoded in the DNA vaccine.

In addition to provide for a danger signal, the versatility of the DNA vaccine design can also be used to optimize antigen processing and presentation to $CD8^+$ T cell receptors by antigen-presenting cells (16). Antigens presented in the context of MHC class I derive from cytosolic proteins, which are degraded after polyubiquitination by the proteasome into peptides (8-11 amino acids) before they are translocated to the endoplasmic reticulum by transporters associated with antigen processing (TAP) for assembly with MHC class I molecules (17). To facilitate proteasomal degradation, antigens can be tagged with sequences encoding ubiquitin leading to improved immune responses against viral (18) and tumor antigens (18, 19).

Based on these considerations, we rationally designed a TH-derived DNA minigene vaccine and show for the first time an ubiquitin-dependent therapeutic antineuroblastoma immune response mediated by mTH-specific $CD8^+$ T cells without induction of autoimmunity using attenuated *S. typhimurium* SL7207 as a vaccine carrier.

Materials and Methods

Three-Dimensional Modeling

Two crystal structures of the murine MHC class I H2-K^k molecule were used for three-dimensional modeling (Protein Data Bank; ref. 20) complexed with octapeptide (Protein Data Bank code *1zt1*) and nonapeptide (Protein Data Bank code *1zt7*; ref. 21), respectively. Structures *1zt1* and *1zt7* were used as the basis for modeling of octamer and nonamer peptides, respectively. The visualization and modeling software Swiss-PdbViewer (22) was used to replace the side chains of the original peptide in structure *1zt1* by those of the mTH-derived peptides 1 to 6 and the alternative epitopes 8 and 9 isolated from NXS2 H2-K^k complexes, whereas *1zt7* was treated the same way for modeling the alternative epitope 7 (Fig. 1A). For this purpose, the software scans a rotamer library to identify the best-fitting side-chain conformation. Steric clashes of the replaced side chains with the protein were removed afterwards.

Subsequently, the docking software GOLD (23) was used to assess binding of the peptides to H2-K^k antigen. The GOLD software optimizes the conformation of the ligand peptide by a so-called simplexing procedure to achieve a maximum score. Logean et al. developed a scoring function, called Fresno, specifically to estimate free energy of binding of peptides to MHC class I molecules (24). This scoring function was incorporated into GOLD by altering the original parameters.

For verification, the three-dimensional structure of the influenza virus HA2-derived peptide FELTGNLI [t], with the highest reported SYFPEITHI score (25) for MHC class I antigen binding (26), was modeled in the same way.

Design and Construction of DNA Minigene Vaccines

Minigenes were constructed by overlapping PCR and cloned into the mammalian expression vector pCMV-F3Ub (kindly provided by J. Whitton and F. Rodriguez, The Scripps Research Institute; ref. 27) using a *Bgl*II restriction site downstream of mutated ubiquitin (Ala^{76}; ref. 18).

The first minigene (altern) was designed as a positive control using the sequence of three natural MHC class I peptide ligands isolated from NXS2 murine neuroblastoma cells (Fig. 1A). These epitopes were identified by immunoprecipitation of MHC class I antigens from NXS2 cells. Peptides were eluted from the precipitate and analyzed by tandem mass spectrometry, which revealed three MHC class I peptide ligands: TEALPVKLI from ribonucleotide reductase M2, NEYIMSLI from serine/threonine protein phosphatase 2A, and FEMVSTLI with unknown origin (27).

The second and third minigenes (mTH3, mTHlow) were selected according to results obtained from SYFPEITHI, comprising three epitopes derived from the protein sequence of mTH with high and low binding affinities to MHC class I H2-K^k antigen (Fig. 1A), respectively.

The minigene design included separation of each epitope by an AAY spacer sequence for each of the constructs, which was shown to be a preferential proteasomal cleavage site (28). All minigenes were supplied with the DNA coding sequence for a hemagglutinin tag, added at the 3′-end of the whole minigene, to allow detection of protein expression.

The crucial role of a stable ubiquitin-peptide transition for the vaccination effect was tested by the generation of the vector pCMV-F3Ub encoding the wild-type ubiquitin by mutation of the COOH-terminal amino acid Ala^{76} back to Gly^{76} using site-directed mutagenesis [GCA (Ala^{76}) to GGA (Gly^{76}); QuikChange Site-Directed Mutagenesis Kit; Stratagene]. The sequences of all constructs in this report were verified by molecular sequencing.

DNA Vaccine Delivery

Attenuated *S. typhimurium* strain SL7207 (AroA-) kindly provided by Dr. B.A.D. Stocker was used for the delivery of DNA vaccines. For this purpose, a single SL7207 colony was grown in Luria-Bertani medium and middle log-phase bacteria were washed twice with ice-cold water. Bacterial cells (1×10^8) were admixed with 0.5 μg plasmid DNA. Electroporation was done in the Eppendorf Multiporator at 2 kV, 25 μF, and 200 Ω for 0.5 s. Cells were immediately

A

origin	MHC class I epitope	*syfpeithi* score	Fresno score
Influenza HA2	[t] FELTGNLI	28	–34.5
Tyrosine hydroxylase = **mTH3**	[1] FETFEAKI*	24	–29.1
	[2] EERDGNAV	22	–24.9
	[3] VEYTKEEI	21	–27.0
Tyrosine hydroxylase = **mTHlow**	[4] HHLETRPA	3	–22.1
	[5] PRKVSELD*	3	–21.5
	[6] QFSQDIGL*	0	–12.4
Ribonucleotide reductase	[7] TEALPVKLI	27	–19.8
Unknown	[8] FEMVSTLI	26	–31.3
Ser/Thr protein phosphatase = **alternative epitopes**	[9] NEYIMSLI	22	–28.4

B

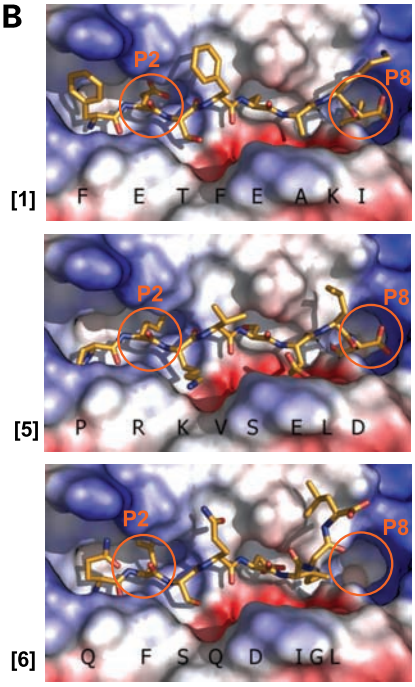

Figure 1. Identification of TH peptides used for DNA minigene vaccine design. TH peptides 1 to 6 were identified by SYFPEITHI and Fresno scores. **A,** these calculated scores assess binding of the peptides to MHC class I H2-K^k antigen. SYFPEITHI scores are based on the peptide sequence only. Fresno scores were calculated after three-dimensional modeling, estimating free binding energies given in kJ/mol. Values for well-characterized influenza virus HA2 peptide [t] (26) and isolated H2-K^k NXS2 neuroblastoma peptides 7 to 9. *Asterisks*, peptides visualized in **B. B,** three-dimensional models of MHC class I H2-K^k peptide complexes 1, 5, and 6. Peptide 1 represents the most affine mTH-derived H2-K^k binder according to SYFPEITHI and Fresno scoring (*top*). Peptides 5 and 6 are low-affinity TH peptides and their three-dimensional H2-K^k peptide complexes are shown (*bottom*). *Orange circles*, anchor positions of amino acids in the H2-K^k molecule, P2 and P8. Both peptides 5 and 6 H2-K^k complexes reveal disturbed peptide binding caused by poor fitting of NH_2-terminal proline into the binding pocket [5] and by a distorted anchor position P8 [6].

covered with 600 μL SOC medium (Invitrogen) and incubated for 45 min at 37°C. A sample of 100 μL was plated onto Luria-Bertani plates containing 50 μg/mL ampicillin (Sigma). Resistant colonies containing the DNA minigene vaccines were cultured and stored after confirmation of the DNA sequence. Mice ($n = 6$) were immunized by oral gavage of SL7207 bacteria growing in middle log phase and carrying the vaccines and control plasmids as depicted in Figs. 2 and 4.

Cells and Mice

NXS2 murine neuroblastoma cells (29) and COS-7 cells were grown in high-glucose DMEM (PAA Laboratories). SCK murine mammary carcinoma and YAC1 cells were grown in RPMI 1640 (PAA Laboratories). All media were supplemented with 10% FCS (PAA Laboratories) and 100 μg/mL penicillin-streptomycin (Invitrogen). Syngeneic female A/J mice were obtained at 6 to 8 weeks of age from Harlan-Winkelmann. The NXS2 model was used as described previously (29). Briefly, primary tumors were induced by s.c. injection of 2×10^6 NXS2 cells and primary tumor growth analyzed by microcaliper measurements. The tumor volume was calculated according to the formula: 1/2 width × length × width. When primary tumors reached a volume of 500 mm^3 on average and/or showed signs of necrosis, they were surgically removed and their weights were determined. Spontaneous liver metastasis was determined at indicated time points after removal of primary tumors by measurements of liver weights, counts of metastatic nodules on the liver surface, and scoring the metastatic load according to 0% = 0, <20% = 1, 20% to 50% = 2, and >50% = 3. All animal experiments were done according to the German Guide for the Care and Use of Laboratory Animals (''Tierschutzgesetz''). Animal experiments were repeated at least once. Data are representative results from one experiment.

Immunohistochemistry

Infiltration of primary tumors, adrenal glands, hearts, kidneys, ovaries, and lungs by T cells was analyzed by immunohistochemistry using anti-CD8 antibody (53-6.7) and anti-CD4 antibody (RM4-5; BD PharMingen) as described previously (30). Expression of TH in adrenergic tissue cryosections of the adrenal glands was determined using rabbit anti-TH antibody (AB152; Chemicon-Millipore). The average number of infiltrating T cells was quantified by light microscopy analyzing 10 high-power fields at a magnification of ×400.

Cytotoxicity Assay

At indicated time points, splenocytes were harvested and incubated in the presence of irradiated NXS2 neuroblastoma cells in RPMI 1640 [10% FCS, 100 μg/mL penicillin-streptomycin, 50 μmol/L β-mercaptoethanol (Sigma), and 100 units/mL interleukin-2] at a ratio of 100:1 for 5 days.

The target cells used were (*a*) NXS2, (*b*) SCK cells pulsed *in vitro* with three mTH3 peptides (FETFEAKI, EERDGNAV, and VEYTKEEI), (*c*) SCK cell controls, and (*d*) YAC1 cell controls. Pulsing was accomplished by incubation of 2×10^6 SCK cells with the three peptides (0.1 μg/mL of each peptide; 24 h, 37°C). Before use, cells were washed once with serum-free medium. CTL activity was determined by using a standard ^{51}Cr release assay. Briefly, 2×10^6 target cells were labeled (2 h, 37°C) with 0.5 mCi ^{51}Cr (1 mCi/mL sodium chromate; Perkin-Elmer) in a total volume of 2 mL and washed three times with complete DMEM. Target cells were plated out at 5,000 per well in a 96-well plate. Effector cells were added to triplicate wells at varying E:T ratios. Samples were taken after 4 and 8 h of incubation, and released radioactivity was determined in a γ-counter (1470 Wizard, Wallace; Perkin-Elmer). Maximum release was induced by incubation of labeled target cells with 5 μL of a 10% SDS solution. Cytotoxicity was calculated according to lysis (%) = [experimental release (cpm) - spontaneous release (cpm)] / [maximum release (cpm) - spontaneous release (cpm)] × 100 (%).

Statistics

The statistical significance of differential findings between experimental groups was determined by nonparametrical Kruskal-Wallis test and further analyzed by the Mann-Whitney *U* test. Findings were regarded as significant if *P* values were <0.05.

Results

Rational DNA Vaccine Design Translates into an Effective Induction of an Antitumor Immune Response

We rationally designed minigene DNA vaccines encoding peptides derived from the entire mTH protein sequence. Peptide selection was based on high affinity to MHC class I antigen molecules as determined by the prediction algorithm SYFPEITHI (25) and high free energy of binding as estimated by the Fresno score (Fig. 1; ref. 24). To compare the two prediction strategies, high-affinity [1-3] and low-affinity [4-6] TH peptides were identified by SYFPEITHI and used to generate three dimensional peptide-MHC class I complex computer models. From these complexes, the free energy of binding was estimated by calculating the respective Fresno scores (Fig. 1). Interestingly, the Fresno scores of low- and high-affinity TH peptides correlated well with SYFPEITHI scores. This result was confirmed by control peptide [t] derived from influenza virus HA2 and alternative octapeptides 8 and 9 from NXS2 neuroblastoma cells. Only peptide 7 TEALPVKLI differs from this trend, supposedly because it is the only nonapeptide in the data set (Fig. 1A).

Inspection of the three-dimensional MHC class I-peptide complexes revealed that all peptides spatially fit into the binding cleft of the MHC molecule (Fig. 1B). During the modeling process, steric clashes occurred at main anchor position P2 for peptides 4 to 6 but not for peptides 1 to 3. Steric clashes of peptides 4 to 6 could be removed by forcing the side chains to adopt unfavored conformations. Results of this process are shown exemplarily for peptides 5 and 6 (Fig. 1B). Forcing peptide 6 to fit into anchor position P2 distorts the structure in such a way that its COOH-terminus protrudes from the MHC class I binding groove, severely disturbing binding at anchor position P8 (Fig. 1B). Inspection of peptide 5 in the MHC class I complex revealed that the NH_2-terminal proline fits poorly into the binding pocket when compared with the NH_2-terminal amino acids of high affinity peptides, which explains the low affinity of peptide 5 to MHC class I antigen H2-K^k (Fig. 1B).

In summary, results of three-dimensional modeling and calculated Fresno scores further support epitope selection by SYFPEITHI delineating peptides 1 to 3 as good candidates for active immunization and peptides 4 to 6 as negative controls.

To test whether these predictions correlate with the induction of an tumor antigen-specific immune response, the MHC class I epitopes were used to generate DNA minigene vaccines (mTH3, mTH3low, alternative epitopes) and evaluated in a syngeneic mouse neuroblastoma model. The minigene vaccines were cloned into the pCMV-F3Ub vector followed by oral delivery with attenuated *S. typhimurium* SL7207 in a prophylactic setting (Fig. 2A; refs. 27, 31). Importantly, the minigene DNA vaccine encoding mTH-derived epitopes with high predicted binding affinity and high free energy of binding to MHC class I (mTH3) effectively induced an antineuroblastoma immune response (Fig. 2B and C). This was indicated by a reduction of the primary tumor growth rate and suppression of spontaneous liver metastasis. This finding was in contrast to that obtained with mice immunized with mTH3low, which was completely ineffective. The vaccination effect of mTH3 was similar to results obtained with the alternative epitope DNA vaccine used as a positive control. These findings were supported by histologic staining of livers from all experimental groups, revealing a complete absence of tumor cells in the mTH3 and the alternative DNA vaccine groups (Fig. 2D).

Role of Ubiquitin in Efficacious DNA Minigene Vaccination

To test the role of a stable minigene-ubiquitin fusion peptide for DNA vaccine efficacy, both mTH3 and alternative minigenes were cloned into the mutated (Ala^{76}) and the wild-type (Gly^{76}) ubiquitin vector, respectively, and tested as oral vaccines *in vivo* (Fig. 3). Only minigene vaccines based on the mutated ubiquitin vector (Ala^{76}) were able to prevent liver metastasis *in vivo*. In contrast, this effect was completely abrogated in mice immunized with DNA vaccines based on wild-type ubiquitin (Gly^{76}). These results emphasize the important role of a stable minigene-ubiquitin fusion peptide providing for proteasomal degradation and subsequent presentation in context with MHC class I antigens.

Therapeutic Vaccination against Neuroblastoma with the mTH3-DNA Minigene

The efficacy of the mutated (Ala^{76}) mTH3-DNA vaccine to induce an antitumor immune response was also tested

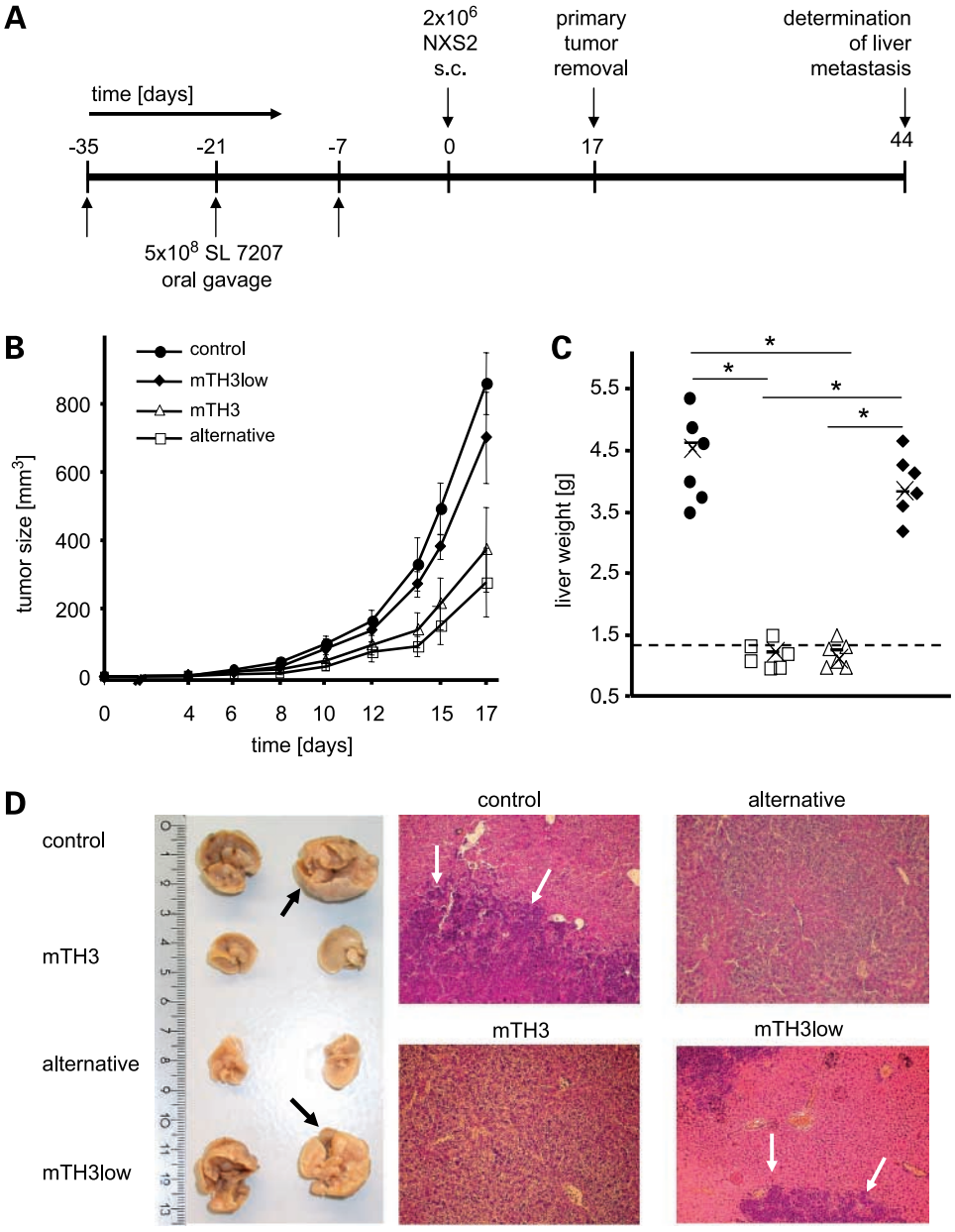

Figure 2. Antineuroblastoma immune response induced by DNA minigene vaccines encoding good or poor MHC class I binding mTH peptides. **A,** schematic of prophylactic vaccination. Three oral vaccinations with 5×10^8 plasmid-bearing attenuated *S. typhimurium* were applied at 2-wk intervals into A/J mice ($n = 6$). Tumor cell injection (s.c. 2×10^6 NXS2 neuroblastoma cells), primary tumor removal, and determination of liver metastasis were done at the time points indicated. **B,** primary tumor growth was measured for 17 d until surgical tumor removal. **C,** spontaneous liver metastasis was determined by measurements of liver weights of fresh specimens. Mean ± SE. *, $P \leq 0.05$. *Horizontal line,* normal liver weights of mice without metastases (1.2-1.4 g). **D,** *left,* photographs of representative liver specimen from each group of mice. *Black arrows,* liver metastases. *Right,* livers were sectioned and tumor cell infiltration was determined by H&E staining. *White arrows,* regions of tumor cell infiltration.

in a therapeutic setting with established neuroblastoma 5 days after tumor cell injection. Vaccines were applied on days 5, 12, 21, 31, and 41 (Fig. 4A) and followed by the determination of spontaneous liver metastases. Due to the aggressiveness of the NXS2 neuroblastoma model, the therapeutic vaccination schedule was intensified compared with prophylactic vaccination. The growth rate of established primary tumors was inhibited by the mTH3 and alternative epitope minigene DNA vaccine in contrast to the untreated control group (Fig. 4B). Importantly, therapeutic vaccination induced the suppression of spontaneous liver metastasis in mTH3 and alternative epitope vaccine groups in contrast to controls (Fig. 4C and D).

Analysis of Infiltrating T Cells in Tissues Expressing TH

To further characterize the immune response following mTH3 minigene DNA vaccination, primary tumor tissue was analyzed by immunohistochemistry (Fig. 5A). Infiltration by both $CD4^+$ and $CD8^+$ T cells into primary tumors was clearly shown in tumor-bearing mice immunized with mTH3 as indicated by an 8-fold increase over the control group (Fig. 5C). Infiltration occurred to a similar extent following DNA vaccination with the alternative epitopes used as a positive control.

In general, autoimmunity is indicated by inflammation followed by tissue necrosis and organ destruction. Analysis of organs by necropsy revealed no macroscopic signs of organ damage caused by autoimmune reactions in all

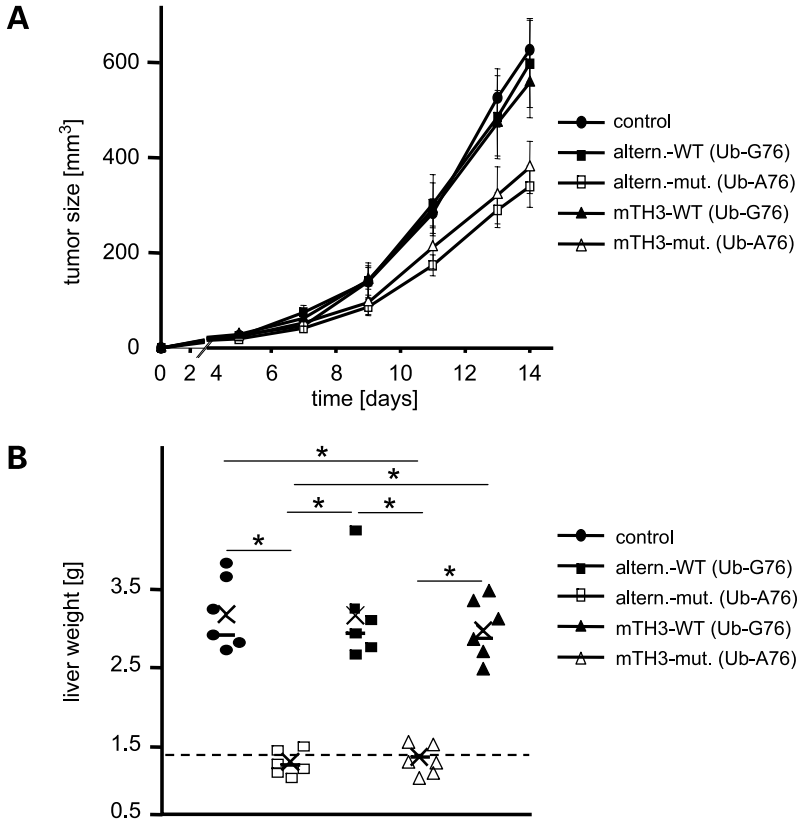

C

	number of tumor nodes on liver surface	grade of liver metastasis
control	250, 250, 250, 250, 250, 250	3, 3, 3, 3, 3, 3
altern. mut.	0, 0, 0, 0, 1, 2	0, 0, 0, 0, 1, 1 ($p<0.05$)
altern. wildtype	250, 250, 250, 250, 100, 100	3, 3, 3, 3, 3, 3
mTH3 mut.	0, 0, 0, 0, 2, 3	0, 0, 0, 0, 1, 1 ($p<0.05$)
mTH3 wildtype	250, 250, 250, 250, 150, 100	3, 3, 3, 3, 3, 3

Figure 3. Role of stable ubiquitin-minigene fusion in the antineuroblastoma effect of mTH3 DNA minigene vaccines. Mice (n = 6) were immunized according to the prophylactic vaccination scheme shown in Fig. 2A and challenged by s.c. injection of 2×10^6 NXS2 neuroblastoma cells. **A,** primary tumor growth was measured for 14 d until surgical tumor removal. **B,** spontaneous liver metastasis was evaluated by measurement of liver weights of fresh specimens. Controls (●), alternative epitopes (■), and mTH3 (▲) vaccine in wild-type ubiquitin-Gly^{76}-pCMV, alternative epitopes (□), and mTH3 (△) vaccine in mutated ubiquitin-Ala^{76}-pCMV. Mean ± SE. *, $P \leq 0.05$. *Horizontal line,* normal liver weights of mice without metastases (1.2-1.4 g). **C,** metastatic score of livers at the end of the *in vivo* experiment: 0% = 0, <20% = 1, 20-50% = 2, and >50% = 3 (*altern.,* alternative).

treated mice (data not shown). Because TH is also expressed in the adrenal medulla (Fig. 5B, *top*), we analyzed T-cell infiltration in adrenal glands. Importantly, there was no increase in $CD8^+$ T cells infiltrating the adrenal medulla in mTH3-vaccinated mice when compared with control groups (Fig. 5B, *bottom*). When this investigation was extended to heart, kidneys, ovaries, and lungs from mTH3 immunized mice, none of these organs showed detectable infiltrating $CD8^+$ T cells (data not shown). In summary, these findings indicate the absence of autoimmunity following mTH3 DNA minigene vaccination.

Specificity of Antineuroblastoma Immune Response following mTH3 Minigene Vaccination

We first tested the *in vitro* cytotoxic response following mTH3 minigene DNA vaccination. For this purpose, splenocytes from immunized mice were analyzed in a cytotoxicity assay using NXS2 murine neuroblastoma cells as targets. Twenty percent cytotoxicity was observed at an E:T ratio of 100:1, which was three times higher compared to the negative control (Fig. 6B, *top*). In contrast, NK-cell sensitive YAC1 target cells (32, 33) were not lysed by splenocytes from mTH3 immunized mice (Fig. 6B, *bottom*). This finding indicates a cytotoxic activity specific for NXS2 surface antigens, which is further supported by IFN-γ secretion. Only splenocytes from mTH3 vaccinated mice produced ~3-fold higher amounts of IFN-γ compared with splenocytes from the negative control group (Fig. 6A).

To prove that tumor-specific lysis is mediated by the mTH3 DNA minigene vaccine, SCK cells were pulsed with the three mTH3 peptides (FETFEAKI, EERDGNAV, and VEYTKEEI) and then used as target cells. SCK is a mammary carcinoma cell line derived from A/J mice,

which does express MHC class I H2-K^K but not TH (data not shown). Only splenocytes of mice immunized with the mTH3 DNA minigene vaccine effectively lysed mTH3 peptide-pulsed SCK cells, whereas splenocytes from both the alternative epitope vaccine and control groups were incapable of inducing lysis (Fig. 6C, *top*). Finally, the same splenocytes showed no cytotoxic activity against naive SCK cells (Fig. 6C, *bottom*), clearly indicating that the immune response induced by the mTH3 DNA minigene vaccine is antigen specific.

Discussion

Novel therapeutic strategies for the treatment of advanced neuroblastoma are very much needed, because the overall survival rate did not significantly improve over the last two decades despite the introduction of high-dose chemotherapy and autologous blood stem cell transplantation followed by retinoic acid (34). Active immunotherapy with DNA vaccines encoding tumor-associated antigens offers an alternative therapy, which is capable to induce specific and long-lasting immune responses (35, 36). The versatility of DNA allows for the design of multifunctional sequences that can be engineered according to the user's needs (31). To critically evaluate a role for a rationally designed DNA minigene vaccine for the immunotherapy of neuroblastoma, we selected epitopes derived from the entire mTH protein sequence. This selection was based on SYFPEITHI and the Fresno scoring methods, which resulted in the identification of mTH peptides with high (mTH3) or low (mTHlow) binding affinity to MHC class I (Fig. 1).

To test the epitope prediction *in vivo*, mice were administered the mTH3 minigene vaccine resulting in reduced tumor growth and suppression of spontaneous liver metastasis. In contrast, this antitumor effect was not observed when applying the low-affinity mTH minigene vaccine (mTHlow). Interestingly, the Fresno score was less predictive in distinguishing H2-K^k antigen binding peptides from nonbinding ones. Nevertheless, this score has shown the correct trend, and by using all available information, including amino acid sequences and inspection of the three-dimensional models, reliable predictions were possible to provide for the development of an effective DNA minigene vaccine against neuroblastoma.

Furthermore, we could clearly show a crucial role for stable monoubiquitination on the induction of an effective

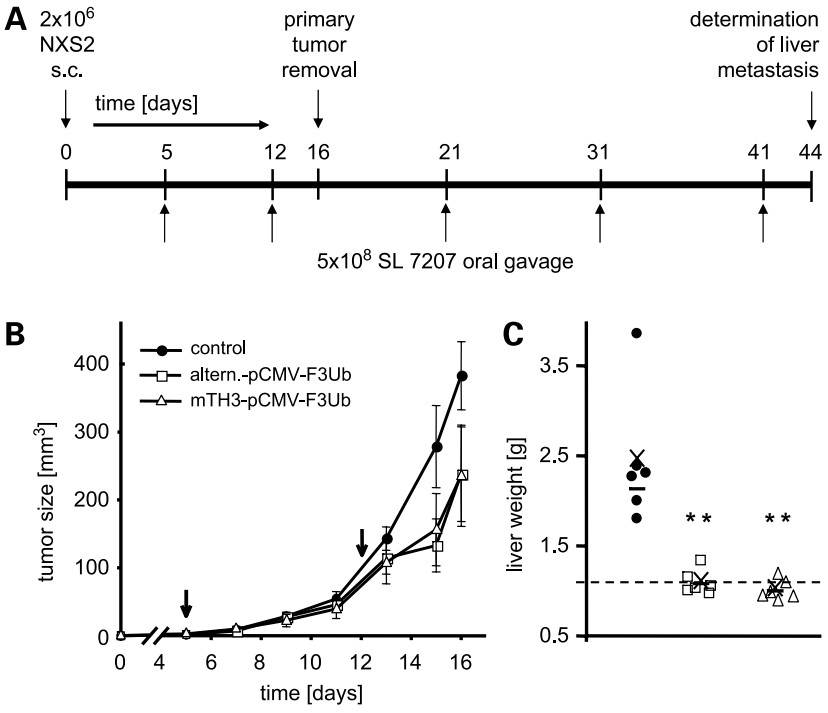

D

	number of tumor nodes on liver surface	grade of liver metastasis
control	250, 250, 250, 250, 250, 250	3, 3, 3, 3, 3, 3
alternative	0, 0, 0, 0, 1, 2	0, 0, 0, 0, 1, 1 ($p<0.05$)
mTH3	0, 0, 0, 0, 2, 3	0, 0, 0, 0, 1, 1 ($p<0.05$)

Figure 4. Therapeutic vaccination against neuroblastoma with the mTH3-DNA minigene. **A,** scheme of therapeutic vaccination. Primary tumors were induced by s.c. injection of 2×10^6 NXS2 neuroblastoma cells ($n = 6$) followed by therapeutic oral vaccinations with plasmid-bearing attenuated *S. typhimurium* starting on day 5 when primary tumors were established. Primary tumor removal and determination of liver metastasis were done at the indicated time points. **B,** primary tumor growth was measured for 16 d until surgical tumor removal. The differences between experimental and control groups were not statistically significant [$P = 0.10$ (alternative epitopes) and $P = 0.21$ (mTH3 epitopes)]. **C,** spontaneous liver metastasis was determined by measurement of liver weights of fresh specimens. Mean ± SE. **, $P \leq 0.01$. *Horizontal line,* normal liver weights of mice without metastases (1.2-1.4 g). **D,** metastatic score of livers at the end of the *in vivo* experiment: 0% = 0, <20% = 1, 20-50% = 2, and >50% = 3.

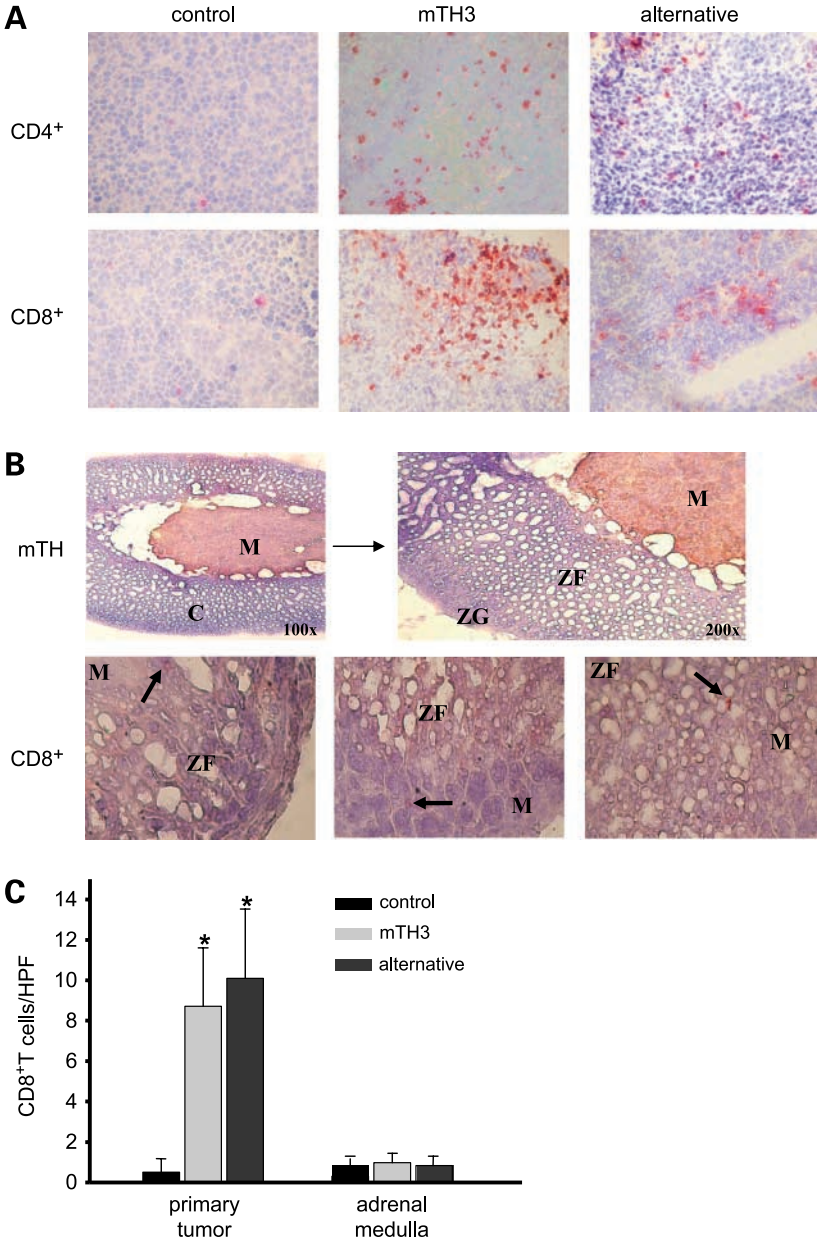

Figure 5. Infiltration of T cells into tissues expressing TH. T-cell infiltration was analyzed by immunohistochemical staining of tumor tissues (**A**) and adrenal glands (**B**). Tissues were frozen and stained with anti-CD4 (**A**, *top*) and anti-CD8 (**A**, *bottom*, and **B**) antibodies. Adrenal glands were additionally stained with anti-TH antibody (**B**, *top*). **A,** *brown,* infiltration by $CD4^+$ and $CD8^+$ T cells. **B,** *top,* TH expression (*brown*) of adrenal medulla (*M*). The adrenal cortex (*C*) can be divided into zona fasciculata (*ZF*) and zona glomerulata (*ZG*). *Bottom, black arrows,* adrenal medulla infiltrating $CD8^+$ T cells. **C,** CD4- and CD8-stained cryosections of tumors and the adrenal medulla were analyzed by light microscopy. Infiltrating $CD4^+$ and $CD8^+$ T cells of 10 fields at a magnification of ×400 were counted. *Columns,* mean of 10 high-power fields; *bars,* SD. The differences in tumor infiltrating $CD8^+$ T cells between groups of mice receiving the mTH3 (*light gray*) and alternative (*dark gray*) vaccines and all control groups (*black*) were statistically significant. *, $P < 0.01$. In contrast, the adrenal medulla was not infiltrated by $CD8^+$ T cells in all immunized animals.

immune response against minigenes (Fig. 3). In fact, it is well known that proteins are subjected to the proteasomal degradation pathway according to the N-end rule (37). However, not all artificially designed minigene peptides will be polyubiquitinated efficiently. Therefore, the mammalian expression vector pCMV-F3Ub was created to ensure stable monoubiquitination of the inserted protein/peptide of interest by mutation of Gly^{76} to Ala^{76}. This mutation was shown to mediate a higher resistance of the ubiquitin fusion peptide to intracellular proteases (38). Similar results were reported for viral antigens and epitopes of carcinoembryonic antigen (19, 39). We extended these findings by comparing for the first time the influence of the COOH-terminal mutation of ubiquitin (Ala^{76}) to wild-type ubiquitin (Gly^{76}) with respect to its antitumor efficacy. Destabilizing the COOH-terminal bond of ubiquitin with the minigene peptide by using the wild-type amino acid Gly^{76} disrupted the ability of the mTH DNA minigene vaccine to induce an antitumor immune response *in vivo*.

The efficacy of this mTH DNA minigene vaccine was also shown in a therapeutic vaccination setting (Fig. 4). The effect on primary tumor growth was relatively weak due to the aggressive nature of the NXS2 neuroblastoma model and the time required to generate a sufficient number of tumor-directed CTLs. Nevertheless, the vaccinated mice presented with a significantly reduced metastasis level in livers and other secondary organs in contrast to control

mice. Thus, once antigen-specific immune cells are activated, they efficiently patrol through the organism in search of their preferred antigen, leading to the deletion of disseminated tumor cells that would finally develop into metastases. This result is encouraging considering the fact that minimal residual disease, the origin of metastases, is a common problem especially in stage IV neuroblastoma where it is concomitant with poor prognosis for the patients (2).

In summary, the advantage of a minigene design is to avoid the use of a whole gene encoding a functional protein with potentially hazardous functions. We showed that the mTH3 minigene vaccine is as effective in inducing an antineuroblastoma immune response as a DNA vaccine encoding the whole mTH cDNA sequence (data not shown). Therefore, the strategy of combining molecular modeling and epitope prediction proved efficacy and might be applicable to other candidate antigen, such as the neuroblastoma-associated oncogene *MYCN*.

The antitumor effect we observed was accompanied by T-cell infiltration of tumor tissue and effector-cell activation as indicated by an 8-fold increase in tumor infiltrating $CD8^+$ T cells (Fig. 5) and a 3-fold elevation in secretion of the T_H1 cytokine IFN-γ (Fig. 6) following mTH3 minigene DNA vaccination in contrast to negative controls. The fact that also $CD4^+$ T cells show an increased infiltration into the tumor microenvironment (Fig. 5A) indicates their role to provide a helper function for the development of a $CD8^+$ T-cell-mediated antitumor immune response. Taken together, these results indicate that tumor-directed CTLs are induced by the mTH3 DNA vaccine. Finally, we could also show antigen specificity of the tumor-directed CTLs *in vitro* (Fig. 6B-D).

Because TH is up-regulated in tissues with high production of catecholamines, e.g., in the adrenal gland medulla, we reasoned that TH-specific CTLs may be found in that location. Interestingly, there was no increase in the number of potentially self-reactive CTLs in mTH3-vaccinated mice compared with the control group (Fig. 5). This encouraging result may be due to the quantity of TH-derived antigenic peptides presented by catecholaminergic cells in the context of MHC class I, which might be too low to be recognized by an activated CTL. Furthermore, CTLs require a signal to leave the vessels and migrate into healthy tissues. Such signals are provided in inflammatory conditions by macrophages producing high amounts of cytokines like tumor necrosis factor-α and/or chemokines. This, in turn, activates endothelial cells to express cellular adhesion molecules like VCAMs or selectins resulting in a microenvironment with the correct ''lymphocyte homing conditions'' (40, 41). In fact, the absence of such lymphocyte homing conditions may protect the adrenal medulla from autoimmunity.

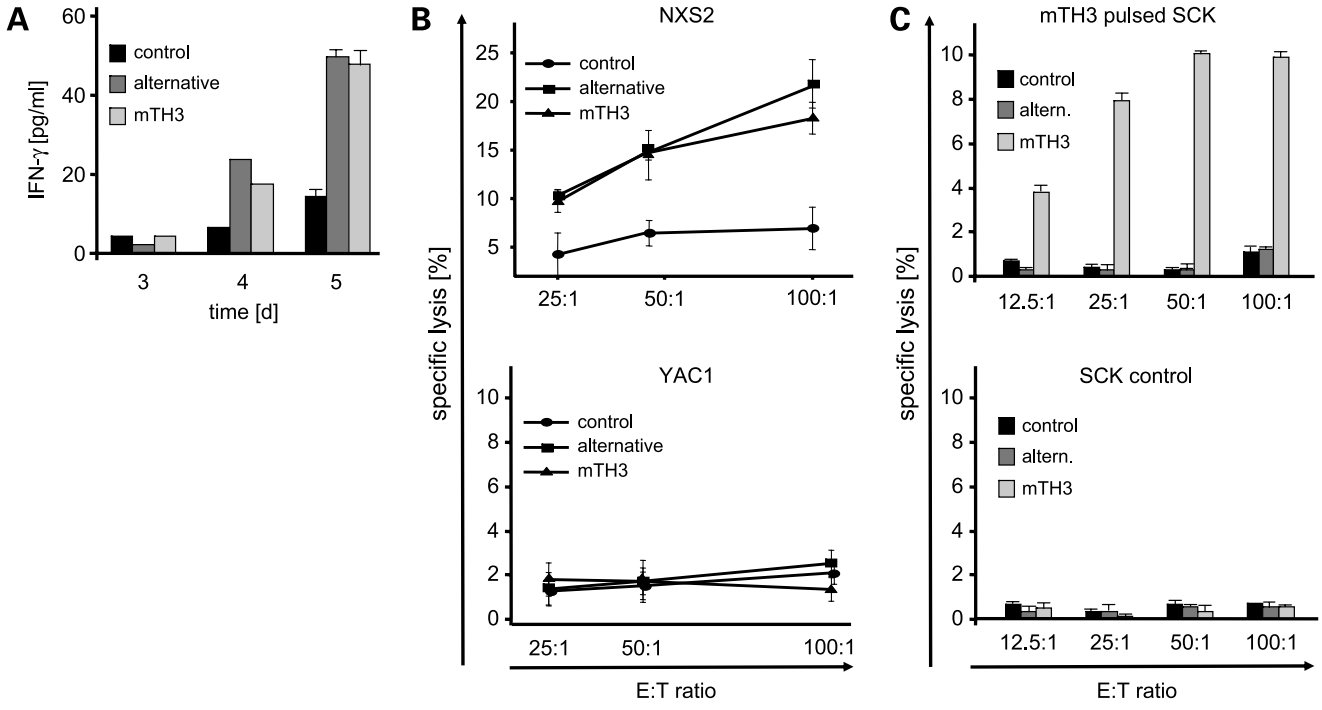

Figure 6. Activation and antigen-specific target cell lysis by T cells following immunization with the mTH3 DNA minigene. Splenocytes harvested from immunized and control mice were stimulated for 5 d in the presence of irradiated NXS2 cells as outlined in Materials and Methods. **A,** IFN-γ concentration was measured by ELISA after 3, 4, and 5 d of stimulation with irradiated NXS2 cells. **B,** for cytotoxicity assay, NXS2 (*top*) or YAC1 (*bottom*) target cells were loaded with ^{51}Cr as described in Materials and Methods. Effector cells were added in different E:T ratios in triplicates. Mean ± SD. **C,** *top,* to show peptide-specific target cell lysis, A/J mammary carcinoma cell line SCK was used as a target. SCK cells were pulsed with mTH3 peptides as described in Materials and Methods and then loaded with ^{51}Cr. Effector cells were added at different E:T ratios in triplicates. Mean ± SD. *Bottom,* as control, naive SCK cells were used as target cells. Effector cells were added at different E:T ratios in triplicates. Mean ± SD.

Treatment strategies of neuroblastoma involving immunotherapy are often considered to be less effective than conventional treatment methods, particularly when they aim for the induction of a CTL-mediated immune response. This is due to the fact that neuroblastoma is a poorly immunogenic tumor and it is still a common opinion among scientists that neuroblastoma is incapable to express MHC class I molecules on its cell surface (42, 43). In fact, MHC class I expression is down-regulated in many neuroblastomas (44, 45). Although the number of MHC class I molecules on neuroblastoma cell surface may be reduced to nearly immeasurable amounts by flow cytometry, a specific lysis by high-affinity CTLs can be induced by only a small number (<10-100) of ligands per cell (46, 47). Furthermore, it was proven that the limited number of MHC class I molecules expressed on a frequently used murine neuroblastoma cell line (C1300) under physiologic conditions was sufficient for an efficient recognition by CTLs (48). The vaccination strategy using attenuated *Salmonella* as a vehicle for DNA vaccines provides for the stimulation of the innate immune system and for a ''danger signal'' (8) associated with the production of cytokines (interleukin-12, IFN-α, and IFN-γ, of which the latter is known to up-regulate MHC class I expression in neuroblastoma cells and other genes encoding necessary subunits of the immunoproteasome; refs. 49, 50).

In summary, we established that a DNA minigene vaccine based on the neuroblastoma-associated antigen TH did successfully induce an antitumor immune response in mice in both prophylactic and therapeutic settings. We could show that this rationally designed mTH3 DNA minigene vaccine, including mutated ubiquitin, induced antigen-specific $CD8^+$ T lymphocytes that effectively inhibited the development of neuroblastoma metastasis *in vivo*. Importantly, potentially self-reactive CTLs induced by our minigene DNA vaccine were not associated with autoimmunity. Considering these results, we believe that a DNA vaccine based on TH may provide a promising new strategy for additional treatment of this challenging tumor in childhood.

Disclosure of Potential Conflicts of Interest

No potential conflicts of interest were disclosed.

Acknowledgments

We thank Prof. Rob Griffin and Brent Williams (University of Minnesota Medical School) for providing an aliquot of SCK cells.

References

1. Simon T, Spitz R, Faldum A, Hero B, Berthold F. New definition of low-risk neuroblastoma using stage, age, and 1p and MYCN status. J Pediatr Hematol Oncol 2004;26:791 – 6.

2. Matthay KK, Villablanca JG, Seeger RC, et al.; Children's Cancer Group. Treatment of high-risk neuroblastoma with intensive chemotherapy, radiotherapy, autologous bone marrow transplantation, and 13-*cis*-retinoic acid. N Engl J Med 1999;341:1165 – 73.

3. Jager E, Jager D, Knuth A. CTL-defined cancer vaccines: perspectives for active immunotherapeutic interventions in minimal residual disease. Cancer Metastasis Rev 1999;18:143 – 50.

4. Stevenson FK, Rice J, Ottensmeier CH, Thirdborough SM, Zhu D. DNA fusion gene vaccines against cancer: from the laboratory to the clinic. Immunol Rev 2004;199:156 – 80.

5. Miyajima Y, Kato K, Numata S, Kudo K, Horibe K. Detection of neuroblastoma cells in bone marrow and peripheral blood at diagnosis by the reverse transcriptase-polymerase chain reaction for tyrosine hydroxylase mRNA. Cancer 1995;75:2757 – 61.

6. Pession A, Libri V, Sartini R, et al. Real-time RT-PCR of tyrosine hydroxylase to detect bone marrow involvement in advanced neuroblastoma. Oncol Rep 2003;10:357 – 62.

7. Engelhard VH, Bullock TN, Colella TA, Sheasley SL, Mullins DW. Antigens derived from melanocyte differentiation proteins: self-tolerance, autoimmunity, and use for cancer immunotherapy. Immunol Rev 2002; 188:136 – 46.

8. Matzinger P. An innate sense of danger. Ann N Y Acad Sci 2002;961: 341 – 2.

9. Donnelly JJ, Wahren B, Liu MA. DNA vaccines: progress and challenges. J Immunol 2005;175:633 – 9.

10. Kutzler MA, Weiner DB. Developing DNA vaccines that call to dendritic cells. J Clin Invest 2004;114:1241 – 4.

11. Hoebe K, Janssen E, Beutler B. The interface between innate and adaptive immunity. Nat Immunol 2004;5:971 – 4.

12. Krieg AM. CpG motifs in bacterial DNA and their immune effects. Annu Rev Immunol 2002;20:709 – 60.

13. Krieg AM. From A to Z on CpG. Trends Immunol 2002;23:64 – 5.

14. Darji A, Guzman CA, Gerstel B, et al. Oral somatic transgene vaccination using attenuated *S. typhimurium*. Cell 1997;91:765 – 75.

15. Cochlovius B, Stassar MJ, Schreurs MW, Benner A, Adema GJ. Oral DNA vaccination: antigen uptake and presentation by dendritic cells elicits protective immunity. Immunol Lett 2002;80:89 – 96.

16. Blankenstein T, Cayeux S, Qin Z. Genetic approaches to cancer immunotherapy. Rev Physiol Biochem Pharmacol 1996;129:1 – 49.

17. Groettrup M, Khan S, Schwarz K, Schmidtke G. Interferon-γ inducible exchanges of 20S proteasome active site subunits: why? Biochimie 2001; 83:367 – 72.

18. Rodriguez F, Zhang J, Whitton JL. DNA immunization: ubiquitination of a viral protein enhances cytotoxic T-lymphocyte induction and antiviral protection but abrogates antibody induction. J Virol 1997;71:8497 – 503.

19. Xiang R, Lode HN, Chao TH, et al. An autologous oral DNA vaccine protects against murine melanoma. Proc Natl Acad Sci U S A 2000;97: 5492 – 7.

20. Berman H, Henrick K, Nakamura H, Markley JL. The worldwide Protein Data Bank (wwPDB): ensuring a single, uniform archive of PDB data. Nucleic Acids Res 2007;35:D301 – 303.

21. Kellenberger C, Roussel A, Malissen B. The H-2Kk MHC peptide-binding groove anchors the backbone of an octameric antigenic peptide in an unprecedented mode. J Immunol 2005;175:3819 – 25.

22. Guex N, Peitsch MC. SWISS-MODEL and the Swiss-PdbViewer: an environment for comparative protein modeling. Electrophoresis 1997;18: 2714 – 23.

23. Verdonk ML, Cole JC, Hartshorn MJ, Murray CW, Taylor RD. Improved protein-ligand docking using GOLD. Proteins 2003;52:609 – 23.

24. Logean A, Sette A, Rognan D. Customized versus universal scoring functions: application to class I MHC-peptide binding free energy predictions. Bioorg Med Chem Lett 2001;11:675 – 9.

25. Rammensee H, Bachmann J, Emmerich NP, Bachor OA, Stevanovic S. SYFPEITHI: database for MHC ligands and peptide motifs. Immunogenetics 1999;50:213 – 9.

26. Stryhn A, Pedersen LO, Romme T, et al. Peptide binding specificity of major histocompatibility complex class I resolved into an array of apparently independent subspecificities: quantitation by peptide libraries and improved prediction of binding. Eur J Immunol 1996;26:1911 – 8.

27. Huebener N, Lange B, Lemmel C, et al. Vaccination with minigenes encoding for novel 'self' antigens are effective in DNA-vaccination against neuroblastoma. Cancer Lett 2003;197:211 – 7.

28. Holzhutter HG, Frommel C, Kloetzel PM. A theoretical approach towards the identification of cleavage-determining amino acid motifs of the 20S proteasome. J Mol Biol 1999;286:1251 – 65.

29. Lode HN, Xiang R, Varki NM, et al. Targeted interleukin-2 therapy for spontaneous neuroblastoma metastases to bone marrow. J Natl Cancer Inst 1997;89:1586 – 94.

30. Lode HN, Xiang R, Dreier T, et al. Natural killer cell-mediated eradication of neuroblastoma metastases to bone marrow by targeted interleukin-2 therapy. Blood 1998;91:1706 – 15.

31. Xiang R, Primus FJ, Ruehlmann JM, et al. A dual-function DNA vaccine encoding carcinoembryonic antigen and CD40 ligand trimer induces T cell-mediated protective immunity against colon cancer in carcinoembryonic antigen-transgenic mice. J Immunol 2001;167:4560 – 5.

32. Kiessling R, Klein E, Wigzell H. ''Natural'' killer cells in the mouse. I. Cytotoxic cells with specificity for mouse Moloney leukemia cells. Specificity and distribution according to genotype. Eur J Immunol 1975;5:112 – 7.

33. Kiessling R, Klein E, Pross H, Wigzell H. ''Natural'' killer cells in the mouse. II. Cytotoxic cells with specificity for mouse Moloney leukemia cells. Characteristics of the killer cell. Eur J Immunol 1975;5:117 – 21.

34. Goldsby RE, Matthay KK. Neuroblastoma: evolving therapies for a disease with many faces. Paediatr Drugs 2004;6:107 – 22.

35. Buchan S, Gronevik E, Mathiesen I, et al. Electroporation as a ''prime/boost'' strategy for naked DNA vaccination against a tumor antigen. J Immunol 2005;174:6292 – 8.

36. Kaplan CD, Kruger JA, Zhou H, et al. A novel DNA vaccine encoding PDGFRβ suppresses growth and dissemination of murine colon, lung and breast carcinoma. Vaccine 2006;24:6994 – 7002.

37. Bachmair A, Finley D, Varshavsky A. *In vivo* half-life of a protein is a function of its amino-terminal residue. Science 1986;234:179 – 86.

38. Ecker DJ, Stadel JM, Butt TR, et al. Increasing gene expression in yeast by fusion to ubiquitin. J Biol Chem 1989;264:7715 – 9.

39. Rodriguez F, An LL, Harkins S, et al. DNA immunization with minigenes: low frequency of memory cytotoxic T lymphocytes and inefficient antiviral protection are rectified by ubiquitination. J Virol 1998;72:5174 – 81.

40. Springer TA. Traffic signals for lymphocyte recirculation and leukocyte emigration: the multistep paradigm. Cell 1994;76:301 – 14.

41. Mackay CR, Andrew DP, Briskin M, Ringler DJ, Butcher EC. Phenotype, and migration properties of three major subsets of tissue homing T cells in sheep. Eur J Immunol 1996;26:2433 – 9.

42. Zier KS, Pierson GR, Brown V. Susceptibility of human neuroblastoma cell lines to cytotoxic T lymphocyte-mediated lysis. J Neuroimmunol 1990;28:153 – 60.

43. Katsanis E, Xu Z, Bausero MA, et al. B7-1 expression decreases tumorigenicity and induces partial systemic immunity to murine neuroblastoma deficient in major histocompatibility complex and costimulatory molecules. Cancer Gene Ther 1995;2:39 – 46.

44. 't Veer LJ, Beijersbergen RL, Bernards R. N-myc suppresses major histocompatibility complex class I gene expression through down-regulation of the p50 subunit of NF-κB. EMBO J 1993;12:195 – 200.

45. Murphy C, Nikodem D, Howcroft K, Weissman JD, Singer DS. Active repression of major histocompatibility complex class I genes in a human neuroblastoma cell line. J Biol Chem 1996;271:30992 – 9.

46. Christinck ER, Luscher MA, Barber BH, Williams DB. Peptide binding to class I MHC on living cells and quantitation of complexes required for CTL lysis. Nature 1991;352:67 – 70.

47. Sykulev Y, Joo M, Vturina I, Tsomides TJ, Eisen HN. Evidence that a single peptide-MHC complex on a target cell can elicit a cytolytic T cell response. Immunity 1996;4:565 – 71.

48. Spierings DC, Agsteribbe E, Wilschut J, Huckriede A. Characterization of antigen-presenting properties of tumour cells using virus-specific cytotoxic T lymphocytes. Br J Cancer 2000;82:1474 – 9.

49. Whitby FG, Masters EI, Kramer L, et al. Structural basis for the activation of 20S proteasomes by 11S regulators. Nature 2000;408:115 – 20.

50. Strehl B, Seifert U, Kruger E, et al. Interferon-γ, the functional plasticity of the ubiquitin-proteasome system, and MHC class I antigen processing. Immunol Rev 2005;207:19 – 30.